CISH targeting in NK cells activates natural cytotoxicity receptor signaling and reduce cell exhaustion to unsilence primary anti-tumor response

Authors: Bernard, P-L. [1], Delconte, R. B. [2,7], Pastor, S. [1], Laletin, V. [1], Goubard, A. [4], Josselin, E. [4], Castellano, R. [4], Vernerey, J. [5], Vivier, E. [6], Huntington, N. D. [2,3], Guittard, G. [1*] and Nunès, J. A. [1*]

*These authors contributed equally

AFFILIATIONS:

[1] Centre de Recherche en Cancérologie de Marseille, CRCM, Immunity and Cancer Team, Institut Paoli-Calmettes, Inserm, CNRS, Aix Marseille Université, Marseille, France.

[2] Department of Biochemistry and Molecular Biology, Biomedicine Discovery Institute, Monash University, Clayton, VIC, Australia.

[3] oNKo-Innate Pty Ltd, Victoria, Australia.

[4] Centre de Recherche en Cancérologie de Marseille, CRCM, TrGET pre-clinical assay platform, Institut Paoli-Calmettes, Inserm, CNRS, Aix Marseille Université, Marseille, France.

[5] Centre de Recherche en Cancérologie de Marseille, CRCM, Plateforme Bioinformatique Intégrative Cibi, Institut Paoli-Calmettes, Inserm, CNRS, Aix Marseille Université, Marseille, France.

[6] Innate Pharma Research Labs, Innate Pharma, Marseille, France; Aix Marseille Université, Inserm, CNRS, Centre d'Immunologie de Marseille-Luminy, CIML, Marseille, France; Service d'Immunologie, Marseille Immunopole, Hôpital de la Timone, Assistance Publique-Hôpitaux de Marseille, Marseille, France.

[7] current address: Immunology Program, Memorial Sloan Kettering Cancer Center, New York, NY, USA.
Correspondence and requests for materials should be addressed to GG geoffrey.guittard@inserm.fr or JAN jacques.nunes@inserm.fr .

Abstract:

Cytokine inducible SH2-containing protein (CISH) is a natural killer (NK) cell negative regulator of cytokine signaling pathway. To further understand-CISH functions in NK cells, we developed a conditional *Cish*-deficient mouse model in NK cells (*Cish*$^{fl/fl}$*Ncr1*$^{Ki/+}$). We detected no developmental or homeostatic differences in NK cells. However, global gene expression of *Cish*$^{fl/fl}$*Ncr1*$^{Ki/+}$ NK cells compared to *Cish*$^{+/+}$*Ncr1*$^{Ki/+}$ NK cells revealed upregulation of pathways and genes associated with NK cell cycling and activation. We show that CISH is not only regulating interleukin-15 (IL-15) signaling pathways but also natural cytotoxicity receptors (NCR) pathways. Indeed, CISH protein expression level increases upon NCR triggering. *Cish*$^{fl/fl}$*Ncr1*$^{Ki/+}$ primed-NK cells showed an increased activation upon NCR stimulation. *Cish*$^{fl/fl}$*Ncr1*$^{Ki/+}$ NK cells display lower activation thresholds and mice are more resistant to tumor metastasis. Remarkably, we found that *Cish*$^{fl/fl}$*Ncr1*$^{Ki/+}$ mice were also more resistant to primary breast cancer growth in addition to superior control of spontaneous tumor metastasis. CISH deletion favors NK cell accumulation to the tumor burden, optimizes NK cell killing properties and decreases TIGIT expression, an immune checkpoint receptor limiting also NK cell

exhaustion. Finally, we argue that specifically enhancing NK cell function is sufficient to boost anti-tumor response to both primary and secondary tumor models, thus validating CISH as a key therapeutic target to enhance NK cell immunotherapy.

INTRODUCTION:

Immunotherapy strategies aim to mobilize the patient's immune defenses against his tumor cells targeting in particular cytotoxic effectors (CD8+ T cells, γδ T cells and natural killer (NK) cells). Antibody-based approaches aim at blocking inhibitory receptors (immune checkpoint inhibitor, ICI) on the surface of cytotoxic cells (CTLA-4, PD-1). These new therapies are mainly targeting $CD8^+$ T cells and have a significant impact on the prognosis and survival of cancer patients. However, many patients are refractory to these treatments. The success and limitations of current immunotherapies have pushed research towards the development of alternative approaches and the possibility to manipulate other cytotoxic immune cells such as Natural Killer (NK) cells.

NK cells receive a renewed interest in immunotherapy because they do not rely on antigen specificity like CD8+ lymphocytes, so they have a broader reactivity to tumors [1,2]. The distinction between a healthy cell (to be spared) and a malignant cell (undesirable) is possible thanks to a panel of inhibitory and activating surface receptors

capable of integrating danger signals. NK cells also play a critical role in helping innate and adaptive immune responses via cellular cross-talk in various disease settings [3]. Finally, in an adoptive transfer therapy setting, NK cells have greater off-the-shelf utility and are safer. Indeed, these cells are less persistent reducing the risk of autoimmunity and side effects such as cytokine storms (CRS, cytokine-release syndrome) that may result from an over activation of T cells. Therefore, therapeutic approaches that trigger and/or reconstitute NK cell function and proliferation are crucial in tumor immunotherapy. In addition, NK cells engineered with CAR, targeting tumor antigens, are highly promising [4].

In numerous preclinical studies, NK cells have shown an ability to limit the metastatic spread of experimental and spontaneous tumors [5,6]. In the clinical setting, NK cell activity has been inversely correlated with cancer incidence [7], and several studies show that NK cell infiltration in lung, gastric, neuroblastoma and colorectal cancers is associated with better patient outcomes [8,9].

Targeting inhibitory intracellular proteins, such as CISH, a member of the SOCS (Suppressor of Cytokine Signaling) family, can be effective in enhancing $CD8^+$ T cell tumor immunity in preclinical models [10,11] these studies led to a clinical protocol NCT04426669. CISH has been also shown to be a critical immune checkpoint in NK cells [12] and we recently contributed to show the importance of CISH in NK cell homeostasis using a *Cish* KO germline mouse model [13]. However, we still do not fully appreciate

mechanistically how CISH regulates NK anti-tumor functions. These are essential requirements to comprehensively uncover the safety of genetically or pharmacologically targeting of an intracellular protein in NK cell immunotherapy.

To further our understanding of NK cell regulation, we developed and investigated a new conditional mouse model that depletes CISH specifically in NK cells (*Cish*$^{fl/fl}$*Ncr1*^{iCre}). In conditional *Cish*-deficient mice (*Cish*$^{fl/fl}$*Ncr1*^{iCre}), we found no homeostatic numbers of NK cells change, no alterations in maturation or cycling. Global gene expression of *Cish*$^{fl/fl}$*Ncr1*^{iCre} NK cells compared to *Cish*$^{+/+}$*Ncr1*^{iCre} NK cells revealed upregulation of pathways and genes associated with NK cell cycling and activation. Indeed, *Cish*$^{fl/fl}$*Ncr1*^{iCre} NK cells displayed a lowered activation threshold upon IL-15 *ex vivo* stimulation. We showed that CISH expression is not only triggered by cytokine stimulation but more unexpectedly upon Natural Cytotoxicity Receptor (NCR) stimulation that are essential for tumor cells recognition. Upon NCR stimulation, we showed enhanced functions and signaling in *Cish*-depleted NK cells. Morevover, *Cish*$^{fl/fl}$*Ncr1*^{iCre} mice were more resistant to experimental tumor metastasis and primary tumor growth. The latter result showing, for the first time, that NK-cell specific deletion of CISH in mature NK cells can dramatically enhance their anti-tumor function in primary tumors. Interestingly, we show that *Cish*-depleted NK cells infiltrated more solid tumor and harbored less inhibiting receptor TIGIT *in vivo* and *ex vivo,* reducing NK cell exhaustion. We conclude that CISH targeting improves NK cell proliferation,

functions, activation of several signaling pathways (cytokines, but also NCRs) and limits NK cell exhaustion. This study represents a crucial step in the mechanistic understanding and safety of targeting *Cish* to unleash NK cell anti-tumor function in solid tumors.

RESULTS

Deletion of CISH in mature NK cells does not impact maturation

To develop a conditional *Cish*-deficient mouse, C57BL/6 germplasm (sperm) were obtained with a Knockout First allele with conditional potential (Cish$^{tm1a(KOMP)Wtsi}$). The EPD0165_3_H07 sperm clone was injected into C57BL/6 female mouse. Mice containing the germline-transmitted Cish^{tm1a} allele were confirmed by PCR and bred to a FLP deleter strain to remove the *lacZ* and *neo*^{r} genes flanked by FLT recognition target sites to generate the floxed *Cish* allele (*Cish*^{tm1cCiphe} or *Cish*$^{fl/fl}$). *Cish*$^{fl/fl}$ mice were then bred with the Ncr1^{iCre} transgenic mice to induce deletion of *Cish* in NK cells (Supplemental Figure 1A). Efficient deletion of CISH was first confirmed by western blot and showed no evidence of CISH in purified and expanded splenic NK cells stimulated with IL-2 or IL-15 (Figure 1B). Similar to germline *Cish*-deleted mice, *Cish*$^{fl/fl}$*Ncr1*^{iCre} mice were healthy, fertile and contained equivalent frequencies and numbers of NK cells in BM and spleen (Supplemental Figure 1A-C).

To determine whether *Cish*-deletion in NK cells perturbs their biology, we assessed the phenotype of NK cells that were deleted of *Cish* from the NKp46^{+} stage

onwards. We did not detect NCRs expression differences nor CD122 (IL-15Rβ) (suppl. Fig 1C). The maturation of *Cish*$^{fl/fl}$*Ncr1*^{iCre} NK cells is normal compared with *Cish*$^{+/+}$*Ncr1*^{iCre} NK cells showing equivalent frequencies of Imm, M1 and M2 populations looking at expression of CD11b and KLRG1 (Figure 1D) or CD27 and CD11b in spleen and BM (Supplemental Figure 1E). We also did not detected differences in DNAM-1 expression in spleen (Figure 1F). Altogether we did not observe any phenotypical differences in *Cish*$^{fl/fl}$*Ncr1*^{iCre} NK cells. This result confirms that targeting CISH is not triggering any adverse effects or modifying NK cells subsets phenotype at steady state. We next decided to compare the genetics of *Cish*$^{+/+}$*Ncr1*^{iCre} and *Cish*$^{fl/fl}$*Ncr1*^{iCre} NK cells.

CISH depletion reveals upregulation of pathways and genes associated with NK cell-cycling and activation

Naïve *Cish*$^{+/+}$*Ncr1*^{iCre} or *Cish*$^{fl/fl}$*Ncr1*^{iCre} cells from spleens were purified and analyzed by RNA seq (Fig.2). After *Cish* deletion, more than 200 genes were differentially expressed (+/- 20% expression, adjusted p-value ⩽ 5%). Among them, about 60 genes have a modulated expression of a factor greater than 2 (Fig.2A). An analysis by KEGG and GO enrichment targeting signaling pathways such as cell cycle progression, cytokine signaling or NK activating receptors, allowed us to assess the influence of the absence of *Cish* on these biological processes and to determine the putative markers responsible for these perturbations (Fig.2 B-D). Overall *Cish*$^{fl/fl}$*Ncr1*^{iCre}

cells appeared to display a more-activated phenotype than their *Cish*$^{+/+}$*Ncr1*^{iCre} counterparts. Subsequently, we decided to evaluate cellular functions of *Cish*-deficient NK cells.

CISH depletion favors IL-15 cytokine signaling pathway decreasing activation threshold

Following IL-15 stimulation, *Cish*-depleted NK cells exhibited an increase proliferation compared to *Cish*$^{+/+}$*Ncr1*^{iCre} cells (Fig. 3A-B). Interestingly, *Cish*$^{fl/fl}$*Ncr1*^{iCre} cells proliferate efficiently at IL-15 doses as low as 10ng/ml, while *Cish*$^{+/+}$*Ncr1*^{iCre} cells are almost not proliferating. We detected no proliferation of *Cish*$^{+/+}$*Ncr1*^{iCre} and *Cish*$^{fl/fl}$*Ncr1*^{iCre} cells at 1ng/ml IL-15 doses, suggesting that *Cish*$^{fl/fl}$*Ncr1*^{iCre} cells can probably proliferate efficiently at IL-15 doses between 1 and 10 ng/ml. *Cish*$^{fl/fl}$*Ncr1*^{iCre} cells showed max proliferation rate at 30ng/ml of IL-15, whereas *Cish*$^{+/+}$*Ncr1*^{iCre} cells needed at least 50ng/ml. These results showing that *Cish*$^{fl/fl}$*Ncr1*^{iCre} NK cells are more sensitive to IL-15 and their activation threshold is greatly diminished in absence of *Cish*. We next decided to follow CD122 (IL-15R) receptor expression during IL-15 activation. CD122 expression remained constant during 6 days in a *Cish*$^{fl/fl}$*Ncr1*^{iCre} context while it decreased in *Cish*$^{+/+}$*Ncr1*^{iCre} at day 3 and Day 6 (Fig. 2C, D). This result suggests a role for CISH in the recycling and degradation of CD122 receptor. We also observed that IL-15-stimulated *Cish*-deficient NK cells showed improved IFN-γ and Cd107a expression. This result correlates with previous results obtained in germline deficient mice [12]. In the absence of

CISH, following cytokine stimulation, there is no negative feedback and NK functions are amplified. The role of CISH under other NK signaling pathways has then been explored.

CISH is expressed upon Natural cytotoxicity receptors stimulation but mildly affected naïve NK cells functions and signaling

We next decided to determine CISH expression upon cytokine stimulation. As expected after 4hrs of IL-2 or IL-15 stimulation we had a great expression of CISH. Interestingly, CISH expression is almost undetectable without stimulation. NK cells express a variety of receptors that allow them to detect target cells (endangered, infected or tumor cells) while sparing normal cells [14]. This recognition is performed via a multitude of activating receptors such as the natural cytotoxicity receptors (NCRs) (NKp30, NKp44, NKp46), NKG2D, 2B4, DNAM-1 or the Fc fragment receptor for immunoglobulins, CD16 (FcRIIA).

The signaling pathways induced by the involvement of TCR (T Cell Receptor) and NCRs (Natural Cytotoxicity Receptors) are very similar[15]. We hypothesized that CISH could intervene in the signal induced by NCR engagement as suggested by our RNA-seq analysis (Fig.2). We showed that CISH can be induced following NKp30 stimulation and NKp46 activating receptors, respectively in a human NK lineage (NK-92) and naive

mouse NK cells (Fig. 4 B-C). These receptors and the integrity of their signaling pathways are essential for the recognition and subsequent elimination of a tumor cell.

The enrichment of genes downstream of activating receptors such as NK1.1, NKp46 and NKG2D, suggests a more activated state of *Cish*-deficient NK cells *in vivo*. We next decided to test NK cells cytokine expression after NCRs activation. Prior to this we confirmed that there is no difference in activating receptor expression on the surface of *Cish*$^{+/+}$*Ncr1*^{iCre} and *Cish*$^{fl/fl}$*Ncr1*^{iCre} NK cells (suppl. Fig 1D). We stimulated naïve *Cish*$^{+/+}$*Ncr1*^{iCre} or *Cish*$^{fl/fl}$*Ncr1*^{iCre} NK cells with plate bound NKp46, NK1.1 or NKG2D antibodies (Figure 4D). We detected no statistical difference in IFN-γ expression, although *Cish*$^{fl/fl}$*Ncr1*^{iCre} cells tend to express more of IFN-γ. The same results were obtained with stronger stimulations such as PMA (phorbol myristate acetate) and ionomycin or IL-12 and IL-18 (suppl.Fig2 A-D). We then decided to explore naïve *Cish*$^{+/+}$*Ncr1*^{iCre} and *Cish*$^{fl/fl}$*Ncr1*^{iCre} NK cells signaling pathway after short NKp46, NK1.1 or NKG2D cross-linking stimulations (Fig4 E, F, G). We decided to use phospho-ERK (p-ERK) antibody that is known to be highly efficient in phosphoflow experiments and known to be activated upon NCR stimulations. We were able to detect a slight increase in p-ERK for all stimulations, confirming the efficient activations of ours cells, but we detected no statistical difference in p-ERK between stimulated *Cish*$^{+/+}$*Ncr1*^{iCre} and *Cish*$^{fl/fl}$*Ncr1*^{iCre} naïve NK cells and even, more ERK phosphorylation at 2 min of NKG2D stimulation of *Cish*$^{+/+}$*Ncr1*^{iCre} NK cells compared to *Cish*$^{fl/fl}$*Ncr1*^{iCre}. We did not detect any

difference as well when stimulating with PMA and Ionomycin (suppl. Fig2.I). Altogether, we conclude, that we do not see major differences in naïve cells NCRs stimulations. We believe this is because CISH is weakly expressed at steady state. Thus we next wanted to test the same stimulations using primed-NK cells.

CISH deletion favors *ex vivo* expanded NK cells proliferation, functions and signaling

To prime our NK cells, we used a process for activation and amplification of splenic murine NK cells (LAKs; Lymphokine-activated killer cells)[16]. Briefly, total splenocytes are cultured in high IL-2 concentration (5000UI/ml). At day 6, we had more total LAKs cells in *Cish*$^{fl/fl}$*Ncr1*^{iCre} compared to *Cish*$^{+/+}$*Ncr1*^{iCre} genotype (Fig 5A). More interestingly, we were able to produce twice the total absolute number of NK cells in *Cish*$^{fl/fl}$*Ncr1*^{iCre} condition compared to *Cish*$^{+/+}$*Ncr1*^{iCre} (Fig 5B). At day 6 post-IL-2 stimulation there are only three kinds of cells remaining, NK cells (NK1.1+, CD3-), NKT cells (NK1.1+, CD3+) and T cells (NK1.1+, CD3-). We observed more production of NK cells and NKT cells in *Cish*$^{fl/fl}$*Ncr1*^{iCre} splenocytes cultures and as a counterpart a dramatic decrease in T cells proportion. NK cells and NKT cells both express NKp46 receptor and are thus Cish-deficient in *Cish*$^{fl/fl}$*Ncr1*^{iCre} mice. Since we showed that Cish-deficient NK cells are more sensitive to cytokine stimulations, this result is in accordance with our previous observations.

We next decided to test whether *Cish*$^{fl/fl}$*Ncr1*^{iCre} NK cells were more sensitive to activating receptor stimulation [NKp46, NK1.1, NKG2D] than their *Cish*$^{+/+}$*Ncr1*^{iCre} counterparts (Fig. 5D). *Cish*$^{fl/fl}$*Ncr1*^{iCre} and *Cish*$^{+/+}$*Ncr1*^{iCre} NK cells from LAKs cultures were stimulated with plate bound NKp46, NK1.1 or NKG2D antibodies. Primed *Cish*$^{fl/fl}$*Ncr1*^{iCre} NK cells showed more expression of IFN-γ especially upon NKP46 and NKG2D stimulations. We then decided to check at primed-NK cells signaling using phosphoflow flow experiments, after short NKp46, NK1.1 or NKG2D cross-linking stimulations (Fig.5 E,F,G). Here again, we were able to see a clear increase in ERK phosphorylation in *Cish*$^{fl/fl}$*Ncr1*^{iCre} NK compared to *Cish*$^{+/+}$*Ncr1*^{iCre} after NCRs stimulation. These observations suggest that the absence of CISH lowers the activation thresholds of these activating receptors by acting on their signaling. This could lead to an increased anti-tumor potential of NK cells in the absence of *Cish*.

Specific deletion of CISH in NK cells enhances immunity to metastasis.

Given the increased activation and proliferation observed *in vitro*, we next asked whether deletion of CISH in NK cells could confer enhanced tumor immunity *in vivo*. We challenged *Cish*$^{fl/fl}$*Ncr1*^{iCre} and *Cish*$^{+/+}$*Ncr1*^{iCre} mice with two syngeneic tumor cell lines, known to be controlled by and stimulate NK cell activity. Intravenous (i.v.) administration of B16F10 melanoma cells showed a decrease in metastatic nodules in the lung compared to *Ncr1*^{iCre} controls (Figure 6A). Similarly, when E0771-GFP/Luc breast cancer cells were administered i.v. to *Cish*$^{fl/fl}$*Ncr1*^{iCre} and *Cish*$^{+/+}$*Ncr1*^{iCre} mice, tumor

burden was significantly reduced at day 7 and 14 in *Cish*$^{fl/fl}$*Ncr1*^{iCre} mice compared to *Cish*$^{+/+}$*Ncr1*^{iCre} mice (Fig.6 B-C). The absence of CISH in NK cells also had an effect on the metastasis of E0771-GFP/Luc breast cancer cells to other organs. Indeed, metastases in the lungs of *Cish*$^{fl/fl}$*Ncr1*^{iCre} mice were significantly decreased compared to *Cish*$^{+/+}$*Ncr1*^{iCre} mice (Fig.6 D). E0771 metastasis to the liver was also measured, with *Cish*$^{fl/fl}$*Ncr1*^{iCre} mice exhibiting significantly reduced metastatic burden (Supplemental Fig. 6E). We next decided to test efficiency of CISH deleted NK cells in a solid tumor model experiment.

Specific deletion of CISH in mature NK cells enhances immunity to primary tumors

NK cells are best defined for their anti-metastatic function. Remarkably, we found that the growth of orthotopic E0771 tumor implanted in the mammary fat pad was also significantly reduced in *Cish*$^{fl/fl}$*Ncr1*^{iCre} mice compared to *Cish*$^{fl/fl}$*Ncr1*^{iCre} mice (Fig. 7A-B). This coincided with reduced spontaneous metastasis to the lungs (Fig.7C-D). We also found more absolute number of infiltrated NK cells in the tumor (Fig.7E). We also checked for activation of these cells, and observed no difference in CD69, CD25 expression, but also no difference in NK cells subtypes (KLRG1, CD11b) present in the tumor when comparing CISH KO NK cells with WT Cells (Suppl. Fig.4 A-D). However, we found a higher expression of CD122 (IL15-Rβ) receptor at the surface of CISH KO NK

cells compared to WT cells (Fig.7F), this correlating our *in vitro* observations. Finally, we checked for checkpoint inhibitors receptors expression at the surface of infiltrated NK cells. Indeed, one of the main causes of relapse in immunotherapy treatment is the exhaustion of cytotoxic cells due to inhibiting receptor expression. We thus tested for PD1, TIM-3 and TIGIT receptors that are all suggested to be a part of NK cells exhaustion (Fig.7G). Interestingly, only TIGIT expression was greatly decreased in infiltrated CISH KO NK cells compared to WT NK cells (Fig7 H-J). We then wanted to see if this observation was confirmed in NK infiltrated in human breast cancer patients. For this, we used previously published Database of Single cells mapping of immunes cells infiltrated in human breast tumors (Azizi et al. Cell 2019). We isolated infiltrated NK cells (*Cd3*-, *Ncam1+)* then observed the expression of *Tigit* comparing *Cish*+ NK cells with *Cish*- cells. Interestingly, we found that *Tigit* is one of the top ten up-regulated gene in presence of *Cish* (fig suppl. 4E) and that *Tigit* gene expression was greatly reduced when *Cish* gene is absent (fig suppl. 4F). This latter result suggests that *Tigit* and *Cish* are regulated similarly in NK cells. We observed in *in vitro* activated NK cells, a similar TIGIT protein downregulation in absence of CISH (suppl. Fig 4G). These data highlight a previously unappreciated role for NK cells in controlling the growth of primary tumors in addition to metastatic cancer cells. We are also showing for the first time, that this efficiency may be the results of several factors especially increased sensitivity to cytokine present in the TME, the tumor cell recognition and less

exhaustion. These data strengthen the rationale for the targeting of CISH in NK cells to improve cancer immunotherapy.

DISCUSSION:

The immunotherapy revolution is ongoing. Many of the current treatments focus on targeting inhibitory cell surface receptors to improve cytotoxic lymphocyte anti-tumor function. Here, we suggest that targeting intracellular "brakes" such as CISH may also be of beneficial interest. Considering the off-target effects of many current immunotherapy treatments, we are mindful of examining the basic biology of targeting intracellular checkpoints alongside the potent anti-tumor responses prior to clinical translation of this strategy. This study explores in detail the effects of depleting CISH in NK cells specifically (*Cish*$^{fl/fl}$*Ncr1*^{iCre}).

Cish-deficient cells are terminally mature and we did not observe any differences in NK cell development in NK cells isolated from *Cish*$^{fl/fl}$*Ncr1*^{iCre} mice compared to WT NK cells. This is contrasting with the maturation defect and DNAM-1 over expression that was found on germline CISH-deleted NK cells [13]. We believe that CISH regulates theses receptors expression processes at an earlier NK cell stage prior to NKp46 expression. Indeed, targeting CISH using CRISPR-Cas9 technology in IPSCs-derived NK cells lead also to a delay in NK cells differentiation [17]. This suggests that targeting CISH in mature NK cells may be a safe strategy in the clinic preventing potential developmental defects.

Our gene set enrichment analysis (GSEA) shows upregulation of signaling pathways essential for NK cell activation and cycling. This observation indicating that in absence of CISH, NK cells are "programmed" to proliferate actively and to be activated. This GSEA allowed us to suggest that CISH may also be a part of other signaling pathways and not only cytokines pathways. Indeed, like we showed in T cell, NK cells increased activation is the result of several signaling pathways i.e. cytokines but also NCR as we show in this study. CISH belong to suppressor of cytokines family (SOCS). We showed in T cells previously and here in NK cells that CISH have a more complex role in cell signaling pathways, we thus believe that probably the other SOCS proteins may have broader effects on signaling as well.

In naïve NK cells we only saw a mild effect of CISH absence functionally. We believe this is due to the fact that CISH is expressed at a very low level at steady state, and will be expressed upon cytokine and or NCR stimulations. This is probably why we had a greater activation of our CISH KO NK cells compared to WT cells, especially after NCR activations. Indeed, we just stimulated one by one these receptors, but in vivo NK cell responses to infectious or tumor cells depend on the balance between several activating and inhibitory signals. Thus, the increased NK cells killing properties observed in absence of CISH is probably the addition of several over activated signaling pathways.

NK cells become more sensitive to their environment due to the decrease in their activation threshold.

It was previously shown that CISH is a potent checkpoint in NK cell-mediated anti-metastatic effect using a CISH germline deficient mouse, *Cish*$^{-/-}$[12]. However, CISH deletion in DC[18], macrophages [19] and T cells[11,20] also favoured the activation of these immune cells. Here, we definitively show that the absence of CISH in NK cells is sufficient to decrease metastasis formation, by using a conditional CISH KO *Cish*$^{fl/fl}$*Ncr1*^{iCre} mouse model. The reduction of tumor metastases in this model emphasizes the importance of NK cells in the anti-tumor response and rules out the role of other immune cells deficient in CISH that may have influenced tumor regression in the germline model.

Previously, an orthotopic injection of E0771 breast cancer cells into germline *Cish*$^{-/-}$ mice resulted in decreased tumour burden and metastasis to other organs [12]. However, there is limited evidence to suggest that the decrease in tumour size is due to increased NK cell function alone, or the orchestration of multiple immune cells lacking CISH (such as CD8 T cells). Strikingly, when *Cish*$^{fl/fl}$*Ncr1*^{iCre} mice were orthotopically implanted with E0771 breast cancer cells, CISH deletion in NK cells alone was enough to decrease tumor burden over time.

We observed more NK cells infiltrated in tumors in absence of CISH. The reason to that is multifactorial, we clearly show here that infiltrated CISH KO NK cells express

more CD122 (IL15-Rβ). One reason to that may be that they are more sensitive to IL-15 and thus may proliferate more efficiently in response to the IL-15 that is present is the tumour microenvironment. We cannot rule out in this study, whether CISH KO NK cells are more efficiently recruited to the tumor site. Further studies are required to test for CISH KO NK cells homing. We also show in here that activated NK cells in absence of CISH are producing more cytokines and degranulating more, especially in response to NCR receptors that are essential for tumor recognition and killing. This means, that these cells are more eager recognize and to kill directly their targets but also probably to influence other immunes cells due to their cytokine's secretion such as DCs and $CD8^+$ T cells. Unexpectedly, we also observed that CISH KO NK cells express less TIGIT that CISH WT cells. TIGIT has been the only one well defined checkpoint inhibitor receptor involved in NK cell exhaustion [21]. This latter result indicates that CISH KO NK cells are less exhausted than their WT counterparts. Further studies are required to understand in detail if TIGIT and CISH are regulating each other expressions or if they are regulated by the same signaling pathways, as it has been suggested for example for IL-15 [22]. Thus, targeting CISH in NK cells represents a promising strategy in immunotherapy not only for anti-metastatic indications but also in primary tumor progression.

The use of human NK cells in adoptive transfer therapy has showed promising results[23]. However, successfully expanding *ex vivo* NK cells to the numbers required for adoptive transfer has been an immense limitation for their use in the clinic[24,25]. We

suggest that engineering human NK cells by deleting CISH may be an interesting strategy to unlock this *ex vivo* proliferation limitation. The CRISPR-Cas9 revolutionizing gene editing tool may be key to this kind of strategy targeting intracellular expressed proteins. We also demonstrate in this study, that in mouse NK cells cultured *in vitro*, the absence of CISH favored NK cell production and increased their sensitivity to cytokines in culture. This may be of interest to optimize human NK cell proliferation protocols.

In conclusion, targeting CISH improves NK cell *ex-vivo* proliferation, functions and signaling activation of several pathways such as cytokines and NCRs. *In vivo* CISH absence favors NK cells number to the tumor burden, otpimize their killing properties and limit NK cell exhaustion.

Thus, in this study we confirmed and further characterized the inhibition of CISH as a method to unleash the NK cell anti-tumor response. We propose that releasing NK cell inhibition by targeting CISH is a safe strategy to improve NK cell anti-tumor properties and supports the clinical development of this approach.

METHODS

Mice:

To generate Tm1c *Cish*$^{fl/fl}$ mice, sperm from *Cish*$^{tm1a(KOMP)WTsi}$ Knock-out mouse project repository (KOMP, UC Davis)[26] was injected into C57BL/6N host embryos at the Centre d'Immunophénomique (Ciphe) (Marseille, France). Homozygous *Cish*$^{tm1a(KOMP)WTsi}$ mice

were then crossed with FLP-FRT mice to generate Tm1c *Cish*$^{fl/fl}$ mice (B6-Cish^{tm1cCiphe}). Then, Tm1c *Cish*$^{fl/fl}$ mice were crossed with *Ncr1*$^{iCre/+}$ mice [27]. Male and female mice were used between the ages of 6–12 weeks. Age and sex matched mice were used and cohort size was dictated by previous experience using these tumor models. Mice were bred and maintained under specific pathogen-free conditions at the Centre de Recherche en Cancérologie de Marseille (CRCM) animal facility. Animal experiments followed were performed in accordance with institutional committees and French and European guidelines for animal care.

Genotyping:

Tm1c *Cish*$^{fl/fl}$ genotyping was performed using the following PCR primers: *Cish* Tm1c Fwd, 5'-GAGGTCTCCCTGAGAACCCC-3'; *Cish* Tm1c Rev, Cis2, 5'-TTCCGCCACTGAGCCACATA-3'; with expected band sizes at 305 bp for WT alleles and 460 bp for floxed allele. *Ncr1*$^{iCre/+}$ genotyping was performed using the following PCR primers: iCRE Fwd, 5'-GGAACTGAAGGCAACTCCTG-3'; iCRE Fwd KI, 5'-GTCCATCCCTGAAATCATGC-3'; Rev WT:-5' TTCCCGGCAACATAAAATAAA-3'; with expected bands sizes at 300 bp for WT allele and 376 bp for KI allele.

NK cell expansion and Western blots

NK cells were purified from mouse spleens using Mouse NK cell isolation Kit according to manufacturer's specifications (STEMCELL #19855). NK cells were then expanded for 6 days with hIL-15 50ng/ml (Miltenyi #130-095-765) in RPMI 20% FCS supplemented with L-glutamine (2 mM; Gibco), penicillin/streptomycin (100 µg/mL; Gibco), Sodium Pyruvate (1 mM; Gibco) and finally FACS sorted (NK1.1^{+}, NKp46^{+}, CD3^{-}, CD19^{-}) (BD Biosciences FACSAria III). After overnight starvation in the absence of IL-15, *Cish*$^{+/+}$*Ncr1*^{iCre} or *Cish*$^{fl/fl}$*Ncr1*^{iCre} NK cells were stimulated or not during 4 hours with IL-2 (Proleukin, Novartis pharma SAS) or IL-15. Cells were lysed at 4 °C for 10 min in 1% NP-40 lysis buffer (50 mM Tris pH 7.4, 150 mM NaCl, 5 mM EDTA, protease inhibitor cocktail (Roche# 11836170001), 1 mM Na3VO4, 0.1% SDS). Samples were resolved by 10% SDS–polyacrylamide gel electrophoresis experiments. Blots were incubated overnight at 4 °C with the corresponding primary antibody directed CISH (Cell Signaling Technology #8731) or Akt (Cell Signaling Technology #9272) for Western blotting. Blots were incubated with horseradish peroxidase–conjugated secondary antibodies (Millipore) for 1 hr at room temperature. ECL (enhanced chemiluminescence; SuperSignal West Pico and SuperSignal West Femto, Pierce) was used to visualize protein bands.

NK cell cytotoxicity assays

Standard 4 hr cytotoxicity assays were completed as described elsewhere[28]. Briefly, splenic NK cells were isolated and suspended in NK cell medium (phenol-red free RPMI 1640 containing 10% FCS, non-essential amino acids, L glutamine and sodium pyruvate, all from Gibco). The indicated target cells were labelled with 15μM Calcein-AM (Life Technologies) for 30 min at 37°C, washed twice and suspended in NK cell medium. Effector and target cells were combined at the indicated ratios in triplicate wells of a round-bottom 96 well plate and incubated at 37°C / 5% CO_2 for 4 hours. Calcein release was quantified by transferring 100 μL of cell-free supernatant to opaque 96 well plates and measuring fluorescent emission at the appropriate wave-length (excitation filter: 485±9 nm; cutoff: 515 nm; emission: 525±15 nm) using the EnVision Robot Plate Reader.

Flow cytometry and cell sorting:

Single-cell suspensions were stained with the appropriate monoclonal antibody in PBS containing 2% FCS. When necessary, intracellular staining was performed by use of the FoxP3/Transcription Factor Staining Buffer Set (eBioscience) according to the manufacturer's instructions. LSRII, Fortessa, (BD Biosciences) were used for cell analysis. Antibodies specific for NK1.1 (PK136; 1:100), CD19 (1D3; 1:400), CD3 (17A2; 1:400 or REA641; Miltenyi Biotec; 1:150); CD122 (TM-β1; 1:200), NKp46 (29A1.4; 1:100), KLRG1 (2F1; 1:200), CD27 (SB/199; 1:200), CD11b (M1/70; 1:200), IL-7R (A7R34;

eBioscience; 1:200) CD49b (DX5; 1:100), CD49a (Ha31/8; 1:200) Ly49H (3D10; 1:200) Ly49D (4E5; 1:200), NKG2D (C4; 1:200), NKG2A/C/E (20d5; 1:200), Ly49C/I (5e6; 1:100), CD107a (104B; 1:100) and IFN-γ (XMG1.2; 1:100), DNAM-1 (10E5; 1:200); Ki-67 (AF488; 1:50) were from BD Pharmingen unless stated otherwise.

Cell Counts:

123count eBeads (BD Bioscience) beads were added to single cell suspensions prior to flow cytometry. Cell numbers were enumerated according to manufacturers instructions.

Enumeration of Apoptotic Cells:

The enumeration of apoptotic cells was performed using the CellEvent™ Caspase-3/7 Green Flow Cytometry Assay Kit (catalogue #: C10427; Thermo Fisher Scientific) following manufacturer's instructions.

Proliferation assay:

For assessment of cellular proliferation by CFSE (carboxy fluorescein diacetate succinimidyl diester; Life Technologies #C34554), splenic NK cells were purified from *Cish* $^{+/+}$*Ncr1*^{iCre} or *Cish*$^{fl/fl}$*Ncr1*^{iCre} mice, then labeled with 0.1 μM CFSE and cultured with various doses of hIL-15 for 5 days, before flow cytometric analysis.

Cytokine assay:

For the measurement of IFN-γ production, splenocytes were activated in 96 well plates with hIL-15 (50 ng/ml), IL-12 (10 ng/ml, Peprotech), IL-18 (100ng/ml), PMA (10ng/ml), Ionomycin (1μg/ml), or coated with anti-NK1.1 (25μg/ml, BioLegend), anti-NKp46 (10μg/ml, BioLegend) or NKG2D (10μg/ml, BioLegend). Cells were incubated with monensin and brefeldin A (BD GolgiPlug and GolgiStop) in complete medium for 4 h at 37°C. The cells were subjected to surface staining and intracellular staining was performed by use of the FoxP3/Transcription Factor Staining Buffer Set (eBioscience).

Tumor cell lines:

B16F10 melanoma cells were obtained from ATCC and were maintained in Dulbecco's Eagle Modified Medium (DMEM) supplemented with 10% FBS. EO771 cell line was purchased from CH3 BioSystems LLC (Amherst, NY, USA). E0771-GFP^{+}-Luciferase were generated as was previously described [29] and were maintained in RPMI-1640 media supplemented with 10% FCS.

Experimental tumor metastasis:

Single-cell suspensions of 3×10^{5} B16F10 melanoma cells were injected i.v. into the tail vein of the indicated strains of mice. Mice were sacrificed and lungs were harvested on day 14. Lungs from B16F10 injected mice were fixed in PFA 4% overnight to count

B16F10 metastases. E0771-GFP$^+$-Luciferase breast cancer cells were injected into the tail vein of the indicated strains of mice (5×10^5 cells/mouse). Luciferase expression was then monitored at day 7 and 14 by bioluminescence using PhotonIMAGER (BiospaceLab), following intraperitoneal injection of luciferin (30 mg/kg). After completion of the analysis organ luminescence was assessed. Orthotopic implantation of breast tumors was performed as previously described [29]. Briefly, EO771-Luc/GFP cells were suspended in 100 µL of a mixture of PBS/Matrigel (v/v) (Corning). 5×10^5 EO771-Luc/GFP cells were injected into the 4th inguinal mammary fat pads of 6 to 10 week old female C57BL/6 mice. Tumor growth was monitored by caliper measurements and weighted at day 15. Lung and liver were harvested at day 15, Luciferase expression was monitored by bioluminescence using PhotonIMAGER (BiospaceLab), after intraperitoneal injection of luciferin (30 mg/kg). Tumor dissociation was performed as previously described [29], the counting of Infiltrated NK cells was performed using countbright absolute counting beads by flow cytometry (ThermoFisher Scientific, #C36950) according to manufacturer's instructions.

Sample preparation, RNA sequencing and bioinformatics analysis:

RNA isolation from sorted *ex vivo* NK cells was extracted using the RNeasy Plus mini Kit (#74134, QIAGEN, Hilden, Germany), according to the manufacturer's instructions. Purified RNA was measured using an Agilent 2200 TapeStation System (Agilent) with

High Sensitivity (HS) RNA ScreenTapes (#5067-5579, Agilent). For Library construction, Full length cDNA were generated from 4 ng of total RNA using Clontech SMART-Seq v4 Ultra Low Input RNA kit for Sequencing (Takara Bio Europe, Saint Germain en Laye, France) according to manufacturer's instructions with 9 cycles of PCR for cDNA amplification by Seq-Amp polymerase. Six hundreds pg of pre-amplified cDNA were then used as input for Tn5 transposon tagmentation by the Nextera XT DNA Library Preparation Kit (96 samples) (Illumina, San Diego, CA) followed by 12 cycles of library amplification. Following purification with Agencourt AMPure XP beads (Beckman-Coulter, Villepinte, France), the size and concentration of libraries were assessed by capillary electrophoresis. The library was sequenced on Illumina Hiseq 4000 sequencer as Single-Read 50 base reads following Illuminas's instruction and base calling were performed using RTA 2.7.7 and bcl2fastq. Approximately 60 million reads per sample were obtained by pooling RNA libraries and performing single-end 50bp sequencing.

Sequencing was performed at the GenomEast platform at the IGBMC (Institut de Génétique et de Biologie Moléculaire et Cellulaire).

Single-End reads 35-76bp in length corresponding to *Cish*$^{-/-}$ and WT *Cish*$^{+/+}$ NK cells (3 biological replicates per group) were quality checked using fastqc[30]. Low quality bases and TrueSeq Adapters were trimmed using trimmomatic[31]. Reads were aligned to mm10 using STAR[32]. The aligned reads were summarized at the gene-level using featureCounts[33]. Genes were filtered from downstream analysis if they failed to achieve

a CPM (counts per million mapped reads) value of at least 0.5 in at least three libraries. Counts were converted to log2-CPM, TMM normalised and precision weighted with the voom function of the limma package[34,35]. A linear model was fitted to each gene and empirical Bayes moderated t-statistics were used to assess differences in expression[36]. Genes were called differentially expressed if they achieved a false discovery rate of 0.05 or less. Differential gene expression analysis, GO and KEGG pathway enrichment analysis were done using the R/Bioconductor package edgeR[37] and limma[34].

ACKNOWLEDGEMENTS

This work is supported in France by institutional grants from the Institut National de la Santé et de la Recherche Médicale (Inserm), Centre National de la Recherche Scientifique (CNRS) and Aix-Marseille Université to CRCM; by project grants from the Fondation ARC pour la recherche sur le Cancer (PJA20161204835), Groupement des Entreprises Françaises dans la Lutte contre le Cancer (GEFLUC) Marseille-Provence, then the Janssen Horizon Fonds de dotation. P-L.B. is supported by a doctoral fellowship from Ligue Nationale contre le Cancer and V.L. by a doctoral fellowship from the Ministère de l'Education et la Recherche. G.G. was supported by a post-doctoral fellowship from the Fondation ARC pour la recherche sur le Cancer and is currently supported by the Janssen Horizon Fonds de dotation. We thank Canceropôle PACA and the Plan Cancer Equipement (#17CQ047-00) for continued support the development of the TrGET

preclinical assay platform. We wish to thank Esma Karkeni for participating in the characterization of the *Cish*$^{fl/fl}$*Ncr1*$^{Ki/+}$ mouse strain and Arnaud Capel for excellent animal husbandry. We are grateful to the staff of the staff of the CRCM animal facility for taking care of the mouse strain colonies and the CRCM cytometry platform for FACS analysis.

AUTHOR CONTRIBUTIONS:

P-L.B., S.P., V.L., A.G.,E.J., R.C., J.V. and G.G. all performed experiments. G.G., and J.A.N. designed experiments and analysed the data. R.B.D.., E.V., and N.D.H. contributed intellectual input and helped to interpret data. G.G. and J.A.N. led the research program. N.D.H., G.G., and J.A.N. wrote the manuscript.

CONFLICTS OF INTEREST

EV is an employee of Innate Pharma and has ownership and stock options. NDH is a founder and share-holder of oNKo-Innate Pty Ltd. NDH receives research funding from Servier, Paranta Biosciences and Anaxis Pharma Pty Ltd.

REFERENCES

1. Shimasaki, N., Jain, A. & Campana, D. NK cells for cancer immunotherapy. *Nat Rev Drug Discov* (2020).
2. Sun, H. & Sun, C. The Rise of NK Cell Checkpoints as Promising Therapeutic Targets in Cancer Immunotherapy. *Front Immunol* **10**, 2354 (2019).
3. Gasteiger, G. & Rudensky, A.Y. Interactions between innate and adaptive lymphocytes. *Nat Rev Immunol* **14**, 631-9 (2014).
4. Liu, E. et al. Use of CAR-Transduced Natural Killer Cells in CD19-Positive Lymphoid Tumors. *N Engl J Med* **382**, 545-553 (2020).
5. Chockley, P.J. et al. Epithelial-mesenchymal transition leads to NK cell-mediated metastasis-specific immunosurveillance in lung cancer. *J Clin Invest* **128**, 1384-1396 (2018).
6. Sathe, P. et al. Innate immunodeficiency following genetic ablation of Mcl1 in natural killer cells. *Nat Commun* **5**, 4539 (2014).
7. Pasero, C. et al. Highly effective NK cells are associated with good prognosis in patients with metastatic prostate cancer. *Oncotarget* **6**, 14360-73 (2015).
8. Souza-Fonseca-Guimaraes, F. NK cell-based immunotherapies: awakening the innate anti-cancer response. *Discov Med* **21**, 197-203 (2016).
9. Shimasaki, N., Jain, A. & Campana, D. NK cells for cancer immunotherapy. *Nat Rev Drug Discov* **19**, 200-218 (2020).
10. Guittard, G. et al. The Cish SH2 domain is essential for PLC-gamma1 regulation in TCR stimulated CD8(+) T cells. *Sci Rep* **8**, 5336 (2018).
11. Palmer, D.C. et al. Cish actively silences TCR signaling in CD8+ T cells to maintain tumor tolerance. *J Exp Med* **212**, 2095-113 (2015).
12. Delconte, R.B. et al. CIS is a potent checkpoint in NK cell-mediated tumor immunity. *Nat Immunol* **17**, 816-24 (2016).
13. Delconte, R.B. et al. NK Cell Priming From Endogenous Homeostatic Signals Is Modulated by CIS. *Front Immunol* **11**, 75 (2020).
14. Pegram, H.J., Andrews, D.M., Smyth, M.J., Darcy, P.K. & Kershaw, M.H. Activating and inhibitory receptors of natural killer cells. *Immunol Cell Biol* **89**, 216-24 (2011).
15. Vivier, E., Nunes, J.A. & Vely, F. Natural killer cell signaling pathways. *Science* **306**, 1517-9 (2004).
16. Viant, C. et al. SHP-1-mediated inhibitory signals promote responsiveness and anti-tumour functions of natural killer cells. *Nat Commun* **5**, 5108 (2014).
17. Zhu, H. et al. Metabolic Reprograming via Deletion of CISH in Human iPSC-Derived NK Cells Promotes In Vivo Persistence and Enhances Anti-tumor Activity. *Cell Stem Cell* **27**, 224-237 e6 (2020).
18. Miah, M.A. et al. CISH is induced during DC development and regulates DC-mediated CTL activation. *Eur J Immunol* **42**, 58-68 (2012).
19. Queval, C.J. et al. Mycobacterium tuberculosis Controls Phagosomal Acidification by Targeting CISH-Mediated Signaling. *Cell Rep* **20**, 3188-3198 (2017).
20. Yang, X.O. et al. The signaling suppressor CIS controls proallergic T cell development and allergic airway inflammation. *Nat Immunol* **14**, 732-40 (2013).
21. Zhang, Q. et al. Blockade of the checkpoint receptor TIGIT prevents NK cell exhaustion and elicits potent anti-tumor immunity. *Nat Immunol* **19**, 723-732 (2018).
22. Villarino, A.V. et al. Subset- and tissue-defined STAT5 thresholds control homeostasis and function of innate lymphoid cells. *J Exp Med* **214**, 2999-3014 (2017).

23. Guillerey, C., Huntington, N.D. & Smyth, M.J. Targeting natural killer cells in cancer immunotherapy. *Nat Immunol* **17**, 1025-36 (2016).
24. Chabannon, C. et al. Manufacturing Natural Killer Cells as Medicinal Products. *Front Immunol* **7**, 504 (2016).
25. Granzin, M. et al. Shaping of Natural Killer Cell Antitumor Activity by Ex Vivo Cultivation. *Front Immunol* **8**, 458 (2017).
26. Skarnes, W.C. et al. A conditional knockout resource for the genome-wide study of mouse gene function. *Nature* **474**, 337-42 (2011).
27. Narni-Mancinelli, E. et al. Fate mapping analysis of lymphoid cells expressing the NKp46 cell surface receptor. *Proc Natl Acad Sci U S A* **108**, 18324-9 (2011).
28. Neri, S., Mariani, E., Meneghetti, A., Cattini, L. & Facchini, A. Calcein-acetyoxymethyl cytotoxicity assay: standardization of a method allowing additional analyses on recovered effector cells and supernatants. *Clin Diagn Lab Immunol* **8**, 1131-5 (2001).
29. Karkeni, E. et al. Vitamin D Controls Tumor Growth and CD8+ T Cell Infiltration in Breast Cancer. *Front Immunol* **10**, 1307 (2019).
30. Andrews, S. FastQC: a quality control tool for high throughput sequence data. (http://www.bioinformatics.babraham.ac.uk/projects/fastqc, 2010).
31. Bolger, A.M., Lohse, M. & Usadel, B. Trimmomatic: a flexible trimmer for Illumina sequence data. *Bioinformatics* **30**, 2114-20 (2014).
32. Dobin, A. et al. STAR: ultrafast universal RNA-seq aligner. *Bioinformatics* **29**, 15-21 (2013).
33. Liao, Y., Smyth, G.K. & Shi, W. featureCounts: an efficient general purpose program for assigning sequence reads to genomic features. *Bioinformatics* **30**, 923-30 (2014).
34. Ritchie, M.E. et al. limma powers differential expression analyses for RNA-sequencing and microarray studies. *Nucleic Acids Res* **43**, e47 (2015).
35. Law, C.W., Chen, Y., Shi, W. & Smyth, G.K. voom: Precision weights unlock linear model analysis tools for RNA-seq read counts. *Genome Biol* **15**, R29 (2014).
36. Smyth, G.K. Linear models and empirical bayes methods for assessing differential expression in microarray experiments. *Stat Appl Genet Mol Biol* **3**, Article3 (2004).
37. Robinson, M.D., McCarthy, D.J. & Smyth, G.K. edgeR: a Bioconductor package for differential expression analysis of digital gene expression data. *Bioinformatics* **26**, 139-40 (2010).

Figure legends:

Figure 1. Deletion of *Cish* gene in mature NK cells does not impact NK cell maturation. (A) Conditional *Cish*-deficient mice were generated by breeding mice containing the germline-transmitted Cish^{tm1a} allele to a FLP deleter strain to remove the *lacZ* and *neo^{r}* genes flanked by FRT recognition target sites. LoxP sites were inserted on either side of exons 2 and 3 to enable Cre-mediated inactivation of the Cish gene in NK cells after breeding to Ncr1^{iCre} mice. (**B**) NK cells were purified from *Cish $^{+/+}$Ncr1$^{Ki/+}$* or *Cish $^{fl/fl}$Ncr1$^{Ki/+}$* spleens, expanded for 6 days with IL-15 and FACS sorted (NK1.1^{+}, NKp46^{+}, CD3^{-}, CD19^{-}). After overnight starvation, *Cish $^{+/+}$Ncr1$^{Ki/+}$* and *Cish $^{fl/fl}$Ncr1$^{Ki/+}$* NK cells were either untreated or stimulated for 4 hours with IL-2 or IL-15. Cell lysates were analysed by immunoblotting for Cish or Akt (loading control). (**C-E)** BM and/or splenic NK cells from *Cish $^{+/+}$Ncr1$^{Ki/+}$* and *Cish $^{fl/fl}$Ncr1$^{Ki/+}$* mice were phenotypically analysed by flow cytometry. (**C**) Frequency of NK cells in spleen and bone marrow (CD3^{-}, CD19^{-}, NK1.1^{+}, NKp46^{+}), representative FACS plots and histograms are shown. (**D**) Frequency of Imm, M1 and M2 cells were measured within NK cell populations from the spleen, representative FACS plots and histograms are shown. (**E**) Frequency of DNAM-1^{+} NK cells and representative histogram is showed.

Figure 2: **CIS depletion reveals upregulation of pathways and genes associated with NK cell cycling and activation.** Gene expression profiles of FACS sorted NK cells (NK1.1^{+}, NKp46^{+}, CD3^{-}) were generated using RNA-sequencing. **(A)** A volcano plot of the top 60 significant (p<0.05) differentially expressed genes with a fold change above +1 or below -1 was generated. y-axis is the negative log-p-value and x-axis is the log-fold-change of the corresponding gene in *Cish*$^{-/-}$ vs *Cish*$^{+/+}$ comparison. Gene expression: blue = downregulated, red = upregulated. **(B-D)** An upregulated list of genes associated with cell cycle **(B)**, cytokine signaling pathways (C) And Natural cytotoxicity receptor pathways (from KEGG pathway analysis) was generated with a p value cut-off of <0.05. x-axis is the log(FC) of each gene and p values are indicated by colour.

Figure 3: Cis depletion favors IL-15 cytokine signaling pathway decreasing activation threshold. **(A-B)** Flow cytometric analysis of *Cish* $^{+/+}$*Ncr1*$^{Ki/+}$ and *Cish* $^{fl/fl}$*Ncr1*$^{Ki/+}$ purified NK cells labeled with carboxyfluorescein succinimidyl ester (CFSE) and cultured for 6 d in IL-15 (10–50 ng/ml). **(A)** Representative FACS plot is showed. **(B)** Representative curve of 3 different experiments are shown. **(C-D)** Flow cytometry was used to quantify the geometric mean of CD122 expression at different time points on *Cish* $^{+/+}$*Ncr1*$^{Ki/+}$ and *Cish* $^{fl/fl}$*Ncr1*$^{Ki/+}$ NK cells. **(C)** Representative curve of 3 different experiments are shown. **(D)** Representative FACS plot is showed. **(E-F)** Histograms of 6 different experiments Flow cytometric analysis of IFN-γ production **(E)** and CD107a

(LAMP-1) **(F)** expression *Cish* $^{+/+}$*Ncr1*$^{Ki/+}$ and *Cish* $^{fl/fl}$*Ncr1*$^{Ki/+}$ NK cells from splenocytes cultured for 4 h in IL-15 (50ng/ml). *p<0.05, **p<0.01 (Student's t-test).

Figure 4: CISH is expressed upon natural cytotoxicity receptors stimulation but mildly affects naïve NK cell functions and signaling. (A-B). Human KHYG-1 NK cells were rested O/N, then stimulated for 4hrs with IL-2 (3000 UI/ml) and IL-15 (50ng/ml) (A), or coated anti-NKp30 antibody (2µg/ml) for the indicated time (B). Cell lysates were analysed by immunoblotting for CISH or AKT (loading control). **(C)** Spleen purified NK cells were stimulated for 4 hours with IL-2 (3000UI/ml) or coated anti-NKp46 antibody. Cell lysates were analysed by immunoblotting for CIS or Akt (loading control). **(D-G)** Total splenic cells were harvested from 6-8 week-old *Cish*$^{+/+}$ and *Cish*$^{-/-}$ mice and depleted of red blood cells. (D-E) Cells were cross-linked with anti-NK1.1, anti-NKp46 and anti-NKG2D coated antibodies for 4 hrs in the absence of IL-15. Flow cytometric analysis of NK cells and their IFN-γ production (D) was assessed after 4 hours. (E-G) Cells were cross-linked with anti-NK1.1, anti-NKp46 and anti-NKG2D coated antibodies for 2, 5 and 10 minutes. Flow cytometric analysis of NK cells ERK1/2 phosphorylation was assessed.

Figure5: Cis deletion favors *ex vivo* expanded NK cells proliferation, functions and signaling. (A-F) Total splenocytes were expanded in IL-2 (1000UI/ml). (A) Histograms

showing absolute numbers of cells that have proliferated at day 6. (B) NK cells gated by FACS (NK1.1+, CD3-) absolute count. (C) FACS gated histogram percentage of NK cells (NK1.1+, CD3-), NKT cells (NK1.1+, CD3+) and T cells (NK1.1-, CD3+). (D-F) After an overnight IL-2-starvation, cells were cross-linked with anti-NK1.1, anti-NKp46 and anti-NKG2D coated antibodies for 4 hrs. Flow cytometric analysis of NK cells and their IFN-γ production (D) was assessed after 4 hrs. (E-G) Cells were cross-linked with anti-NK1.1, anti-NKp46 and anti-NKG2D coated antibodies for 2, 5 and 10 minutes. Flow cytometric analysis of ERK1/2 phosphorylation in NK cells was assessed. $^{*}p<0.05$, $^{**}p<0.01$ (Student's *t*-test).

Figure 6: Specific deletion of CIS in NK cells enhances immunity to metastasis. **(A)** 3×10^5 B16F10 melanoma cells were injected i.v. into *Cish* $^{+/+}$*Ncr1*$^{Ki/+}$ and *Cish* $^{fl/fl}$*Ncr1*$^{Ki/+}$ mice and 14 days later lung metastases were enumerated. (**B-C**) 5×10^5 EO771-GFP$^+$ Luciferase$^+$ breast cancer cells were injected i.v. into *Cish* $^{+/+}$*Ncr1*$^{Ki/+}$ and *Cish* $^{fl/fl}$*Ncr1*$^{Ki/+}$ mice and metastatic burden was quantified by luminescence at day 7 (left panel) and 14 (right panel). (C) Representative luminescence pictures are showed. (**D, E**) 5×10^5 EO771-GFP$^+$ Luciferase$^+$ breast cancer cells were injected i.v. into *Cish* $^{+/+}$*Ncr1*$^{Ki/+}$ and *Cish*$^{fl/fl}$*Ncr1*$^{Ki/+}$ mice and spontaneous metastatic burden was quantified by luminescence at day 14 in the lungs (**D**) and liver (**E**). $^{*}p\leqslant0.05$ $^{**}p\leqslant0.01$ $^{***}p\leqslant0.001$ (unpaired Student's *t*-test).

Figure 7: Specific deletion of CIS in mature NK cells enhances immunity to primary tumors (**A-J**) Orthotopic injection of EO771-GFP^{+} Luciferase^{+} breast cancer cells in the mammary fat pad of *Cish* $^{+/+}$*Ncr1*$^{Ki/+}$ and *Cish*$^{fl/fl}$*Ncr1*$^{Ki/+}$ mice. (**A**) Measure of tumor growth in mm^{3} at indicated timepoints. **(B)** Measure of tumor weight at day 15. **(C-D**) At day 15, lungs from tumour bearing *Cish* $^{+/+}$*Ncr1*$^{Ki/+}$ and *Cish*$^{fl/fl}$*Ncr1*$^{Ki/+}$ mice were analysed and metastatic burden quantified by luminescence. **(D)** Pictures of lung luminescence at day 15. **(E)** Numbers of infiltrated NK cells (NK1.1^{+}, CD3^{-}) /mm^{3} of tumors. **(F)** Flow cytometry was used to quantify the mean fluorescence of CD122 expression on Infiltrated NK cells. **(G)** Flow cytometry was used to quantify the mean fluorescence ratio to WT infiltrated NK cells MFI of TIGIT, PD-1, TIM-3 and CD122. **(H-J)** TIGIT expression analysis by flow cytometry. (H) Representative plot comparing *Cish* $^{+/+}$*Ncr1*$^{Ki/+}$ and *Cish*$^{fl/fl}$*Ncr1*$^{Ki/+}$ TIGIT , profile. **(I)** Percentage of TIGIT positive cells and **(J)** Mean fluorescence intensity of TIGIT. Mean ± s.e.m. of $n \geq 9$ biological replicates;.*$p<0.05$, **$p<0.01$, ***$p<0.01$ (Student's *t*-test).

Figure 1

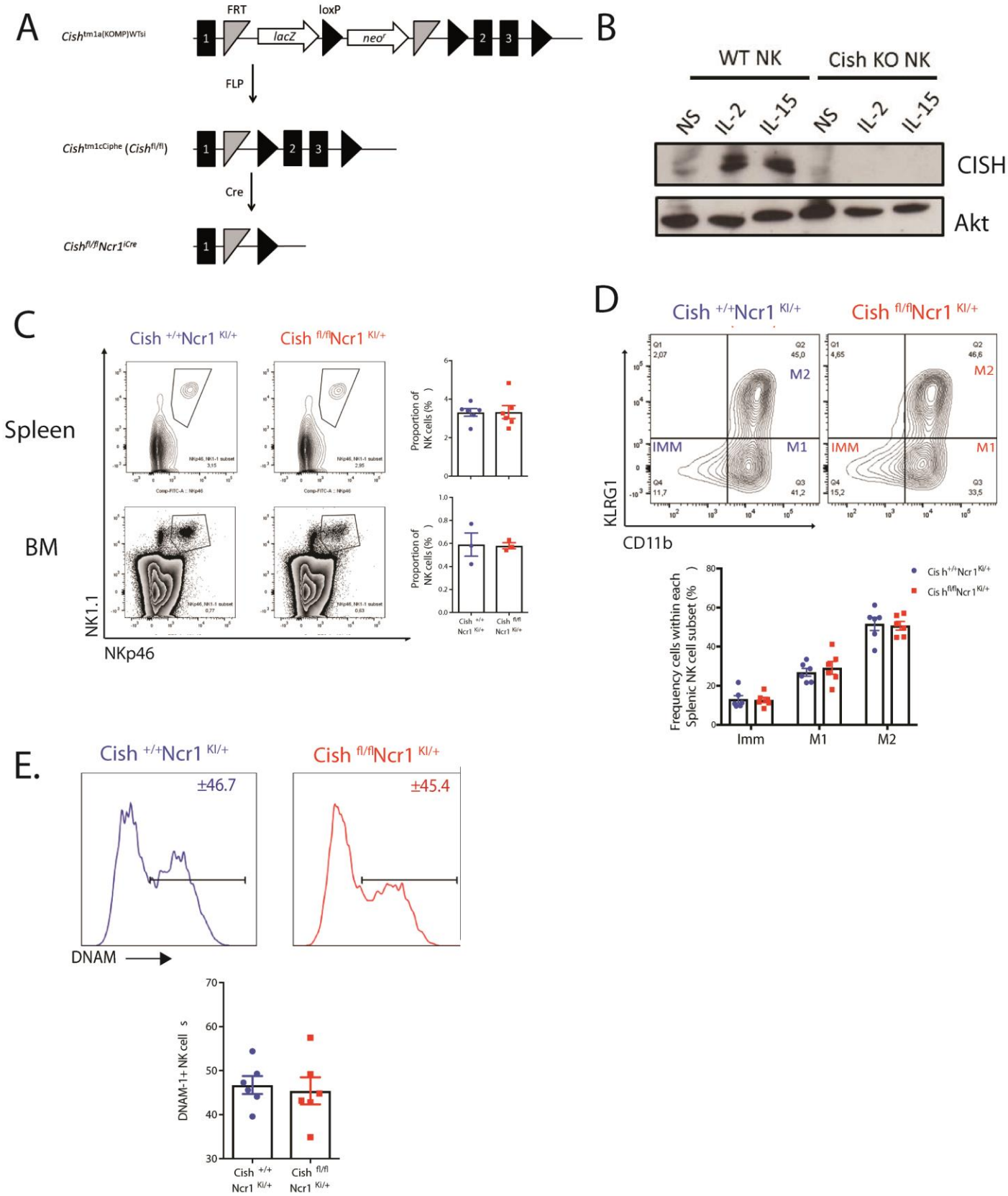
A
Cish tm1a(KOMP)WTsi
FRT
loxP
lacZ
neo r
FLP
Cish tm1cCiphe (Cish fl/fl)
Cre
Cish fl/fl Ncr1 iCre
B
WT NK
Cish KO NK
NS
IL-2
IL-15
CISH
Akt
C
Cish +/+ Ncr1 KI/+
Cish fl/fl Ncr1 KI/+
Spleen
BM
NK1.1
NKp46
Proportion of NK cells (%)
D
KLRG1
CD11b
IMM
M1
M2
Frequency cells within each Splenic NK cell subset (%)
Imm
E.
±46.7
±45.4
DNAM
DNAM-1+ NK cells

Figure 2

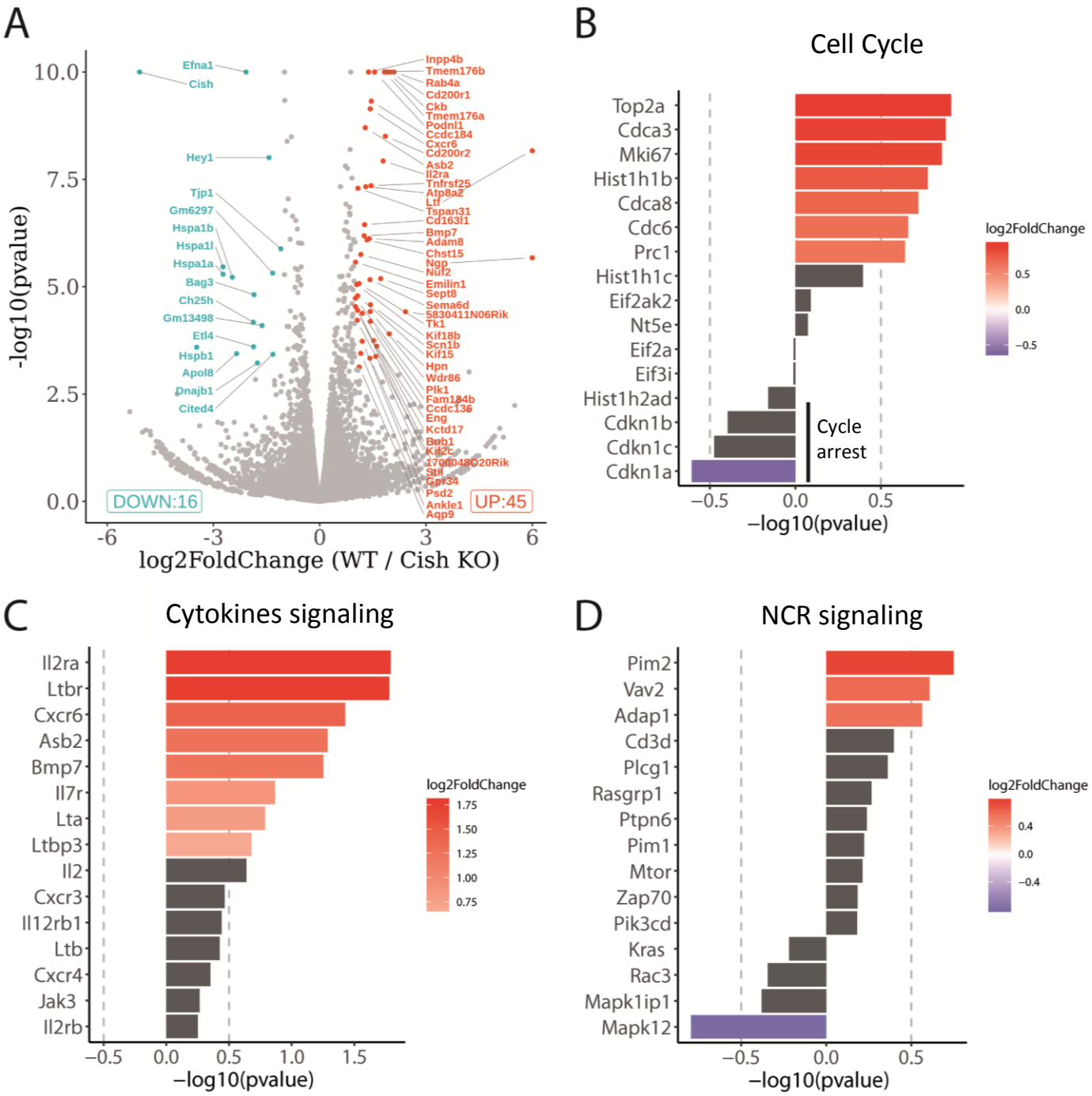
A
-log10(pvalue)
log2FoldChange (WT / Cish KO)
DOWN:16
UP:45
Efna1
Cish
Hey1
Tjp1
Gm6297
Hspa1b
Hspa1l
Hspa1a
Bag3
Ch25h
Gm13498
Etl4
Hspb1
Apol8
Dnajb1
Cited4
Inpp4b
Tmem176b
Rab4a
Cd200r1
Ckb
Tmem176a
Podnl1
Ccdc184
Cxcr6
Cd200r2
Asb2
Il2ra
Tnfrsf25
Atp8a2
Ltf
Tspan31
Cd163l1
Bmp7
Adam8
Chst15
Ngp
Nuf2
Emilin1
Sept8
Sema6d
5830411N06Rik
Tk1
Kif18b
Scn1b
Kif15
Hpn
Wdr86
Plk1
Fam184b
Ccdc136
Eng
Kctd17
Bub1
Kif2c
1700048O20Rik
Stil
Gpr34
Psd2
Ankle1
Aqp9
B
Cell Cycle
Top2a
Cdca3
Mki67
Hist1h1b
Cdca8
Cdc6
Prc1
Hist1h1c
Eif2ak2
Nt5e
Eif2a
Eif3i
Hist1h2ad
Cdkn1b
Cdkn1c
Cdkn1a
Cycle arrest
log2FoldChange
−log10(pvalue)
C
Cytokines signaling
Il2ra
Ltbr
Cxcr6
Asb2
Bmp7
Il7r
Lta
Ltbp3
Il2
Cxcr3
Il12rb1
Ltb
Cxcr4
Jak3
Il2rb
log2FoldChange
−log10(pvalue)
D
NCR signaling
Pim2
Vav2
Adap1
Cd3d
Plcg1
Rasgrp1
Ptpn6
Pim1
Mtor
Zap70
Pik3cd
Kras
Rac3
Mapk1ip1
Mapk12
log2FoldChange
−log10(pvalue)

Figure 3

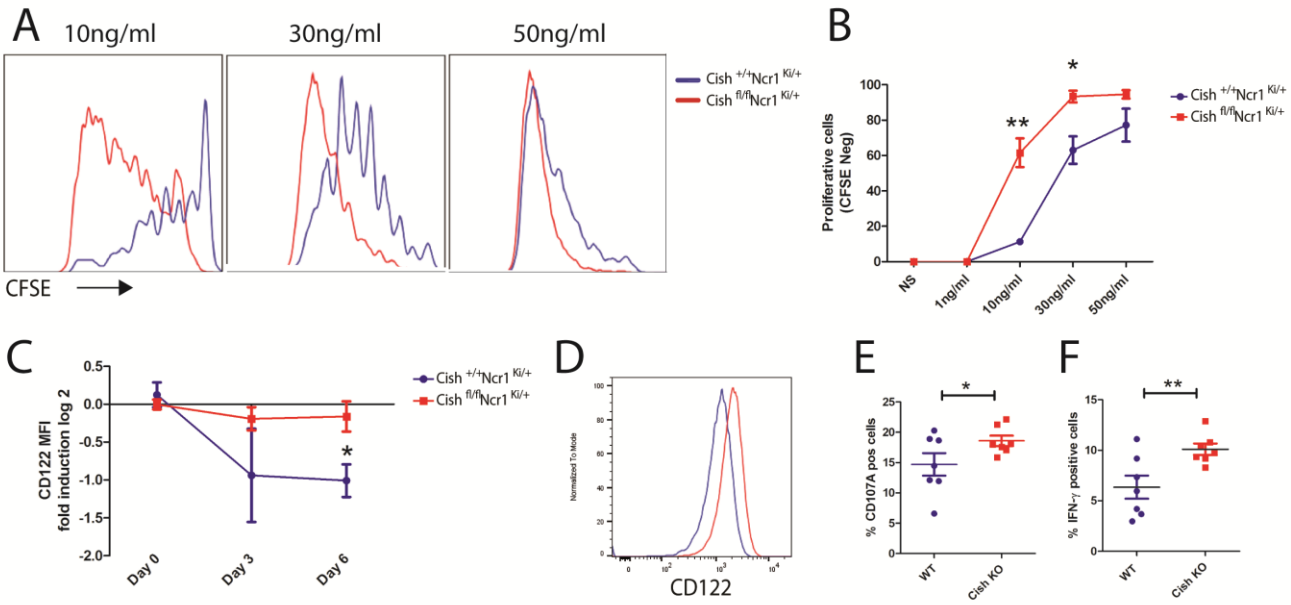
A
10ng/ml
30ng/ml
50ng/ml
Cish +/+Ncr1 Ki/+
Cish fl/flNcr1 Ki/+
CFSE
B
Proliferative cells (CFSE Neg)
NS
1ng/ml
10ng/ml
30ng/ml
50ng/ml
C
CD122 MFI fold induction log 2
Day 0
Day 3
Day 6
D
Normalized To Mode
CD122
E
% CD107A pos cells
WT
Cish KO
F
% IFN-γ positive cells
WT
Cish KO

Figure 4

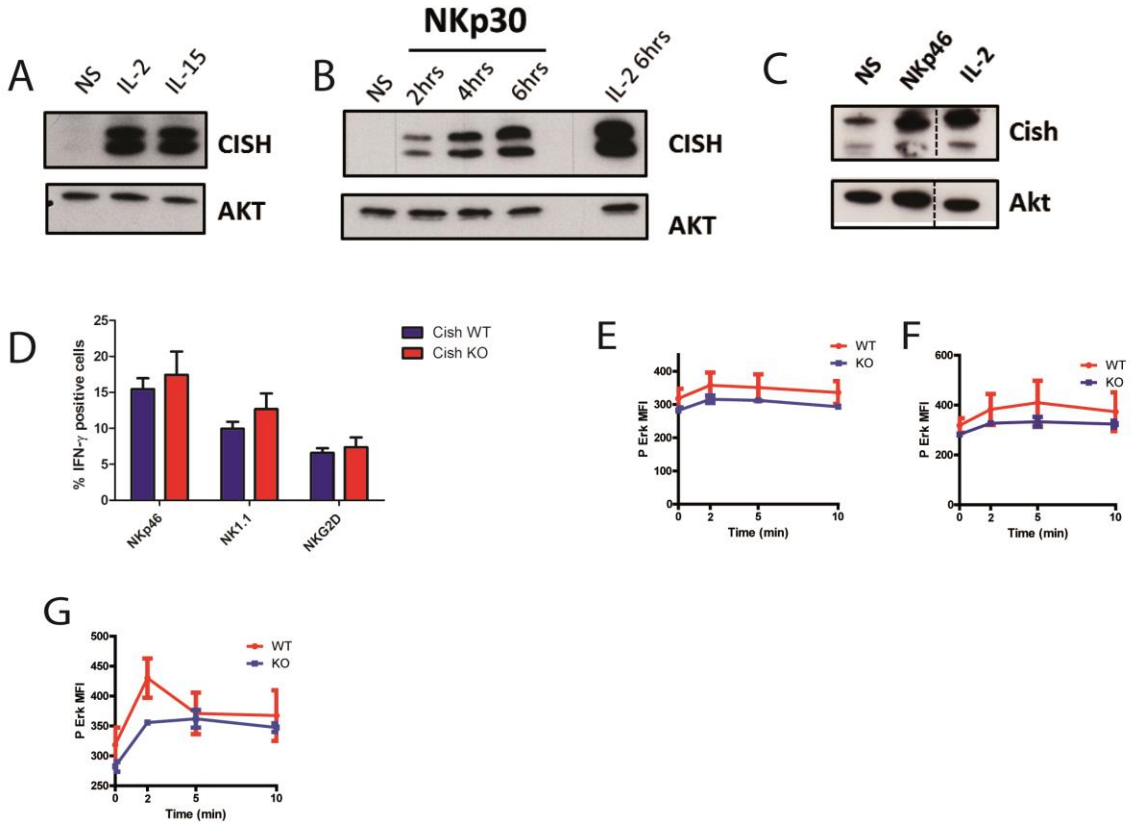
A
NS
IL-2
IL-15
CISH
AKT
B
NKp30
NS
2hrs
4hrs
6hrs
IL-2 6hrs
CISH
AKT
C
NS
NKp46
IL-2
Cish
Akt
D
% IFN-γ positive cells
Cish WT
Cish KO
NKp46
NK1.1
NKG2D
E
WT
KO
P Erk MFI
Time (min)
F
WT
KO
P Erk MFI
Time (min)
G
WT
KO
P Erk MFI
Time (min)

Figure 5

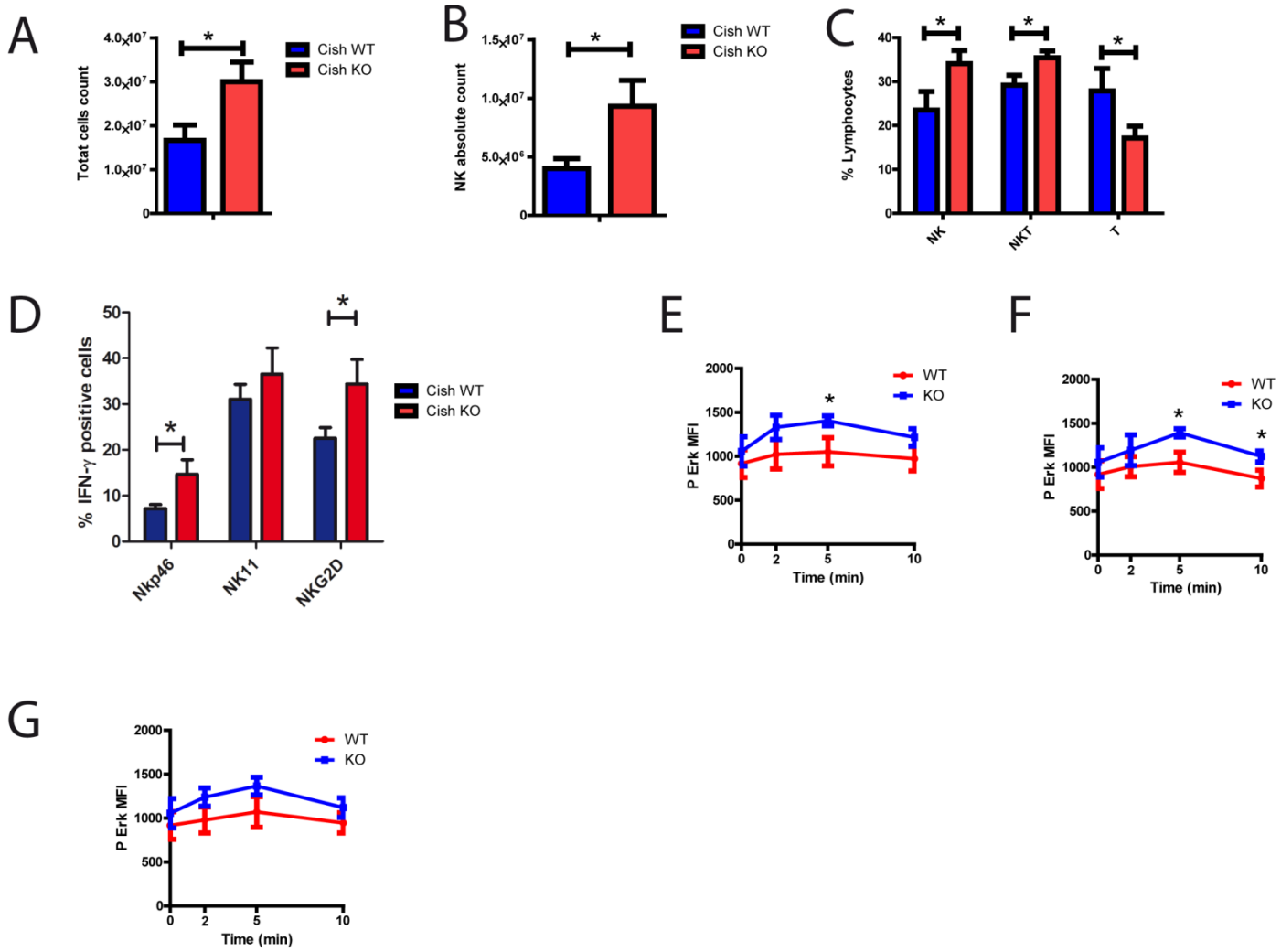
A
Totat cells count
4.0x10^7
3.0x10^7
2.0x10^7
1.0x10^7
0
*
Cish WT
Cish KO
B
NK absolute count
1.5x10^7
1.0x10^7
5.0x10^6
0
*
Cish WT
Cish KO
C
% Lymphocytes
40
30
20
10
0
*
*
*
NK
NKT
T
D
% IFN-γ positive cells
50
40
30
20
10
0
*
*
Nkp46
NK11
NKG2D
Cish WT
Cish KO
E
P Erk MFI
2000
1500
1000
500
0
*
WT
KO
0
2
5
10
Time (min)
F
P Erk MFI
2000
1500
1000
500
0
*
*
WT
KO
0
2
5
10
Time (min)
G
P Erk MFI
2000
1500
1000
500
0
WT
KO
0
2
5
10
Time (min)

Figure 6

A

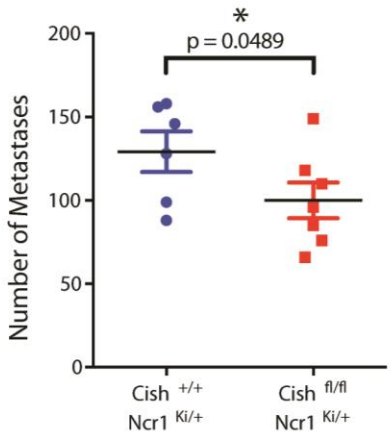

B

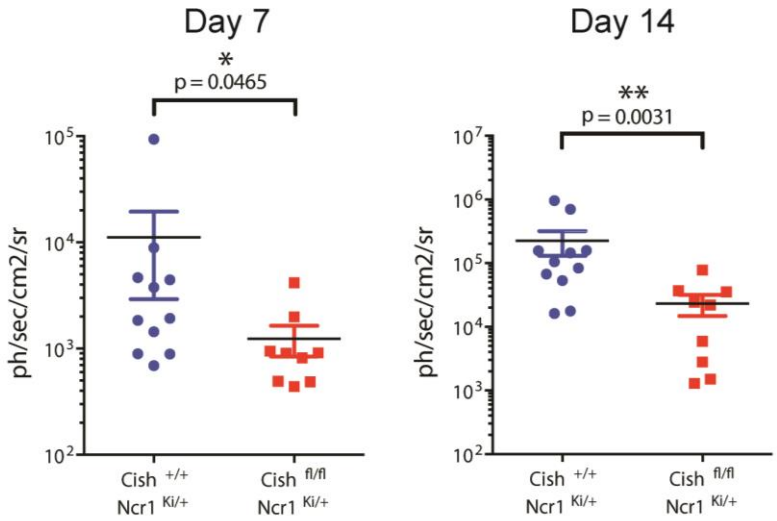

C

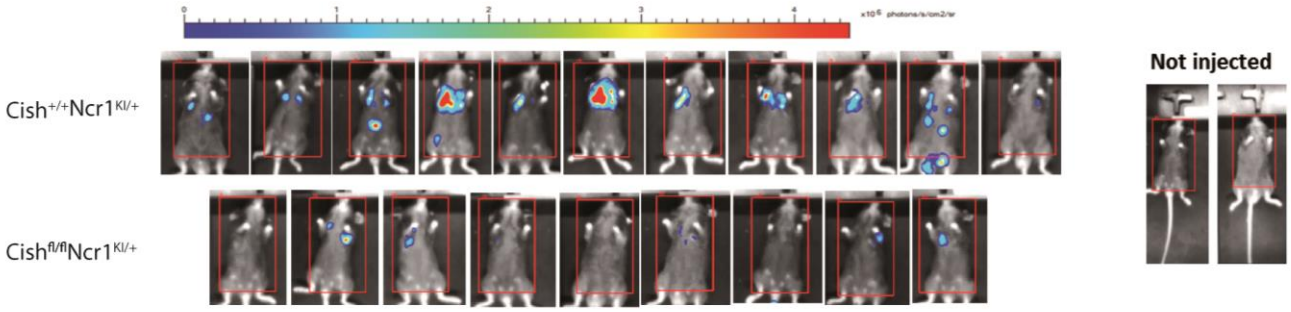

D

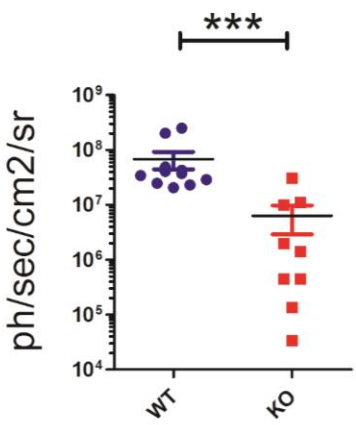

E

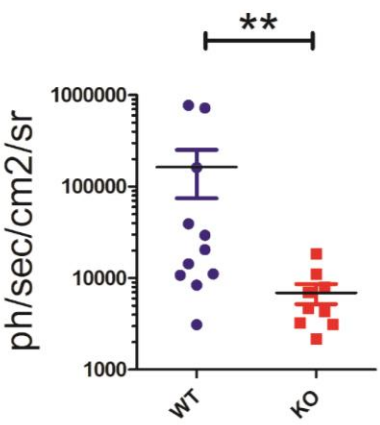

Figure 7

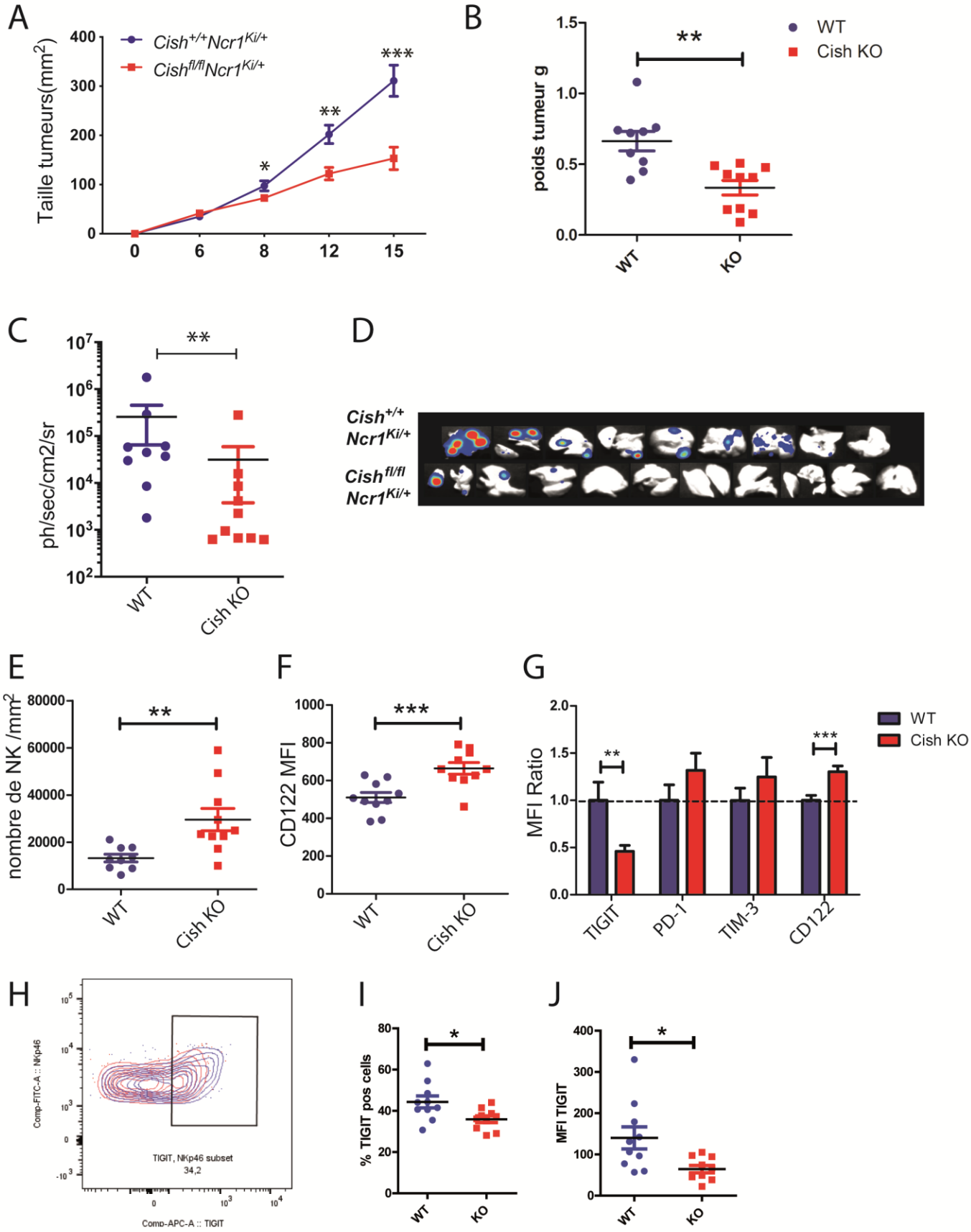
A
Taille tumeurs(mm²)
Cish+/+Ncr1Ki/+
Cishfl/flNcr1Ki/+
*
**
***
B
poids tumeur g
WT
Cish KO
**
C
ph/sec/cm2/sr
**
D
Cish+/+ Ncr1Ki/+
Cishfl/fl Ncr1Ki/+
E
nombre de NK /mm²
**
F
CD122 MFI
***
G
MFI Ratio
WT
Cish KO
**
***
TIGIT
PD-1
TIM-3
CD122
H
Comp-FITC-A :: Nkp46
TIGIT, NKp46 subset
34,2
Comp-APC-A :: TIGIT
I
% TIGIT pos cells
*
J
MFI TIGIT
*